RESOURCE

nature immunology

Translation is actively regulated during the differentiation of CD8+ effector T cells

Koichi Araki[1], Masahiro Morita[2,3,5], Annelise G Bederman[1], Bogumila T Konieczny[1], Haydn T Kissick[1,4], Nahum Sonenberg[2,3] & Rafi Ahmed[1]

Translation is a critical process in protein synthesis, but translational regulation in antigen-specific T cells *in vivo* has not been well defined. Here we have characterized the translatome of virus-specific CD8+ effector T cells (T_{eff} cells) during acute infection of mice with lymphocytic choriomeningitis virus (LCMV). Antigen-specific T cells exerted dynamic translational control of gene expression that correlated with cell proliferation and stimulation via the T cell antigen receptor (TCR). The translation of mRNAs that encode translation machinery, including ribosomal proteins, was upregulated during the T cell clonal-expansion phase, followed by inhibition of the translation of those transcripts when the CD8+ T_{eff} cells stopped dividing just before the contraction phase. That translational suppression was more pronounced in terminal effector cells than in memory precursor cells and was regulated by antigenic stimulation and signals from the kinase mTOR. Our studies show that translation of transcripts encoding ribosomal proteins is regulated during the differentiation of CD8+ T_{eff} cells and might have a role in fate 'decisions' involved in the formation of memory cells.

CD8+ T cells have a crucial role in controlling intracellular infection and anti-tumor immunity. During acute infection, antigen-specific CD8+ naive T cells (T_n cells) proliferate and differentiate into CD8+ T_{eff} cells that eliminate the pathogen-infected cells[1]. The majority of those CD8+ T_{eff} cells die after pathogen clearance, and then the long-lived CD8+ memory T cell (T_m cell) population is formed. The differentiation of CD8+ T_{eff} cells and T_m cells is accompanied by dynamic changes in the phenotype and function of antigen-specific CD8+ T cells, as revealed by genome-wide transcriptomic analyses[2,3]. In addition, it is increasingly apparent that epigenetic regulation is involved in the formation of CD8+ T_{eff} cells and T_m cells[4–7].

In addition to such transcriptional and epigenetic analyses, investigation into the post-transcriptional regulation of antigen-specific CD8+ T cell responses is needed for better understanding of cellular events that occur during the effector and memory differentiation of these cells. Translation is a key target for post-transcriptional regulation, as it is a critical process in the synthesis of proteins from the genetic information encoded in mRNAs[8]. The translational regulation of gene expression is involved in many cellular events, and its dysregulation can result in clinical manifestations, including cancer and mental disorders[9–11]. Translation also has an important role in controlling both innate immune responses and adaptive immune responses[12]. The production of certain cytokines in T_{eff} cells is translationally regulated[13–15]. Distinct translational signatures have been found in Foxp3+ CD4+ regulatory T cells and Foxp3− CD4+ T cells[16]. Translation might also regulate the CD8+ T cell response during antigen-triggered activation in physiological settings such as pathogen infection, vaccination and cancer, because mTOR, a major regulator of translation[17], has an essential role in the differentiation of CD8+ T_{eff} cells and T_m cells[18,19]. However, how the translation of individual mRNAs is regulated in these activated CD8+ T cells has not been studied, and it is unclear if translation changes during the process of differentiation into CD8+ T_{eff} cells and T_m cells.

In this study we have investigated the translational profiles of CD8+ T cells isolated *ex vivo* during acute infection of mice with LCMV. Genome-wide translational analysis indicated that the expression of a group of genes encoding the translational machinery was dynamically regulated by translational mechanisms in activated CD8+ T cells. Furthermore, we found that antigenic stimulation as well as mTOR signals were involved in this translational regulation. Our studies provide a framework for understanding the translational profiling of CD8+ T cells activated *in vivo*.

RESULTS

Activated CD8+ T cells change their translational activity

To define how the translation of mRNA is regulated in activated CD8+ T cells during acute infection, we compared the translation profiles of CD8+ T_n cells, T_{eff} cells and T_m cells using P14 mice, which transgenically express a TCR specific for the H2-D^b-restricted LCMV gp33 epitope. We isolated CD8+ T_n cells from the spleen of uninfected P14 mice. To obtain T_{eff} and T_m cells, we adoptively transferred CD45.1+ P14 CD8+ T_n cells into wild-type (CD45.2+) mice, followed by infection

[1]Emory Vaccine Center and Department of Microbiology and Immunology, Emory University School of Medicine, Atlanta, Georgia, USA. [2]Department of Biochemistry, McGill University, Montreal, Canada. [3]Goodman Cancer Research Centre, McGill University, Montreal, Canada. [4]Department of Urology, Emory University School of Medicine, Atlanta, Georgia, USA. [5]Present address: Department of Molecular Medicine and Barshop Institute for Longevity and Aging Studies, University of Texas Health Science Center at San Antonio, San Antonio, Texas, USA. Correspondence should be addressed to R.A. (rahmed@emory.edu) or K.A. (karaki@emory.edu).

Received 14 March; accepted 16 June; published online 17 July 2017; doi:10.1038/ni.3795

of the host mice with the Armstrong strain (Arm) of LCMV and isolation of P14 $CD8^+$ T cells from spleen at day 5 after infection (D5 T_{eff} cells), day 8 after infection (D8 T_{eff} cells) or 40–60 d after infection (T_m cells). As described previously[20], infection with LCMV Arm resulted in viral clearance at 8 d after infection and substantial expansion of the antigen specific $CD8^+$ T cell population in the spleen, followed by a contraction phase (**Fig. 1a**). $CD8^+$ T_n cells from the spleen of uninfected P14 mice maintained a small cell size, did not proliferate and did not express the cytotoxic molecule granzyme B (**Fig. 1b–d**). On the other hand, D5 T_{eff} cells were larger in size (**Fig. 1b**) and were actively proliferating in response to viral antigens (**Fig. 1a**,**d**). In addition, they expressed granzyme B (**Fig. 1c**). The cell size of $CD8^+$ T_{eff} cells at day 8 after infection (D8 T_{eff} cells), at the peak of the $CD8^+$ T cell response, was comparable to that of $CD8^+$ T_n cells (**Fig. 1b**), and they were not proliferating (**Fig. 1d**) but had high expression of granzyme B (**Fig. 1c**). After the contraction phase, $CD8^+$ T_m cells (>30 d after infection) in spleen were small, did not take up the thymidine analog BrdU, similar to T_n cells and D8 T_{eff} cells, and had lower expression of granzyme B than that of D5 T_{eff} cells or D8 T_{eff} cells (**Fig. 1b–d**).

We next investigated the polysome profiles of $CD8^+$ T_n cells, D5 T_{eff} cells, D8 T_{eff} cells and T_m cells. $CD8^+$ T_n cells, isolated from spleen of uninfected P14 mice and separated by ultracentrifugation on a sucrose gradient, had a lower polysome content than that of the monosome peak (**Fig. 1e**), a result confirmed by the smaller amount of RNA isolated from the polysome fractions than from the monosome fractions in these cells (**Fig. 1e**). These data suggested low translational activity in $CD8^+$ T_n cells, consistent with the status of T_n cells as quiescent cells. In contrast to $CD8^+$ T_n cells, P14 $CD8^+$ D5 T_{eff} cells purified from the spleen of LCMV Arm–infected mice showed multiple distinct spikes in the polysome fractions and a large amount of RNA in these fractions (**Fig. 1e**), indicative of active translation of mRNA during the clonal expansion phase. The polysome profile of P14 $CD8^+$ D8 T_{eff} cells isolated from spleen of LCMV Arm–infected mice at the peak of the T cell response (day 8 after infection) was similar to that of T_n cells (**Fig. 1e**). These results suggested that activated $CD8^+$ T cells downregulated mRNA translation when they stopped dividing (at day 8 after infection). P14 $CD8^+$ T_m cells (isolated from spleen of mice at days 40–60 after infection) had a low polysome content (**Fig. 1e**), which indicated quiescent translation. These polysome-profile data suggested that mRNA translation in $CD8^+$ T cells correlated with cell proliferation.

Next we assessed incorporation of L-homopropargylglycine (HPG)[21,22], a non-radioactive amino-acid analog of methionine that can be measured by flow cytometry[21], to assess protein synthesis in $CD8^+$ T_n cells, T_{eff} cells and T_m cells. Mouse splenocytes were cultured for 2 h at 37 °C with HPG in the presence (as a control) or absence of cycloheximide, an inhibitor of protein synthesis. In accordance with the polysome-profiling data, very few T_n cells incorporated HPG (**Fig. 1f**), indicative of minimal protein synthesis. In contrast, at day 5 after infection, 40% of the T_{eff} cells were HPG^+ (**Fig. 1f**). At day 8 after infection, the frequency of HPG^+ cells was much lower (<10%) among D8 T_{eff} cells than among D5 T_{eff} cells (**Fig. 1f**), and by day 12 after infection, the frequency of HPG^+ cells among antigen-specific $CD8^+$ T cells became similar to that observed among T_n cells (**Fig. 1f**), which indicated that active protein synthesis was transient. Low incorporation of HPG was also seen in T_m cells (**Fig. 1f**). Together these results suggested that protein synthesis increased at day 5 after infection in proliferating antigen-specific $CD8^+$ T cells, followed by a rapid reduction in protein production concurrent with the peak of $CD8^+$ T cell responses at day 8 after infection, as the cells stopped dividing.

Selective translational control of gene expression in $CD8^+$ T cells

To investigate the regulation of the translation of mRNAs known to be expressed in activated $CD8^+$ T cells, we assessed the sedimentation of specific mRNAs across the fractions obtained by sucrose-gradient ultracentrifugation. $CD8^+$ T_n cells were obtained directly from the spleen of P14 mice, and $CD8^+$ T_{eff} cells were isolated from spleen of LCMV Arm-infected mice given adoptive transfer of P14 cells before infection. Translation of *Ifng* mRNA (which encodes interferon-γ (IFN-γ)) is known to be required for the production of IFN-γ protein in T cells activated *in vitro*[13–15]. *Ifng* mRNA was transcriptionally upregulated in both D5 T_{eff} cells and D8 T_{eff} cells relative to its expression in T_n cells (**Fig. 2a**), as shown previously[2,3]. In D5 T_{eff} cells, *Ifng* mRNA was broadly distributed in the sedimentation gradient, and about 40% of the total *Ifng* mRNA was located in polysome fractions, while only about 20% of the total *Ifng* mRNA was detected in polysome fractions in D8 T_{eff} cells (**Fig. 2b**,**c**). It has been shown that the peak of IFN-γ protein in serum and organ homogenates following infection with LCMV occurs before day 8 after infection and that $CD8^+$ T cells are the main contributors to the production of IFN-γ protein[23]. We found that the amount of IFN-γ protein in serum peaked at day 5 after infection with LCMV and then decreased significantly by day 10 after infection (**Fig. 2d**). Direct *ex vivo* intracellular cytokine staining showed that D5 T_{eff} cells produced more IFN-γ than did D8 T_{eff} cells (**Fig. 2e**), consistent with the data on the translation of *Ifng* mRNA; this indicated the translation of *Ifng* mRNA was more active in proliferating activated D5 T_{eff} cells than in D8 T_{eff} cells that had stopped proliferating.

We also assessed the translation of *Tbx21* mRNA (which encodes the transcription factor T-bet). The expression of *Tbx21* mRNA was induced in D5 T_{eff} cells and D8 T_{eff} cells relative to its expression in T_n cells (**Fig. 2f**). However, in contrast to results obtained for *Ifng* mRNA, there was no difference between D5 T_{eff} cells and D8 T_{eff} cells in their translation of *Tbx21* mRNA (**Fig. 2g**,**h**), and about 80% of the total *Tbx21* mRNA was detected in polysomes in both D5 T_{eff} cells and D8 T_{eff} cells (**Fig. 2h**), which indicated that the translation of *Tbx21* mRNA in activated T_{eff} cells was more efficient and stable than that of *Ifng*.

Cd8a mRNA (which encodes the co-receptor CD8α) was constitutively expressed in $CD8^+$ T cells through all activation and differentiation stages (**Supplementary Fig. 1a**). 50–70% of the total *Cd8a* mRNA was found in polysome fractions of all subsets of $CD8^+$ T cells examined (T_n cells, D5 T_{eff} cells, D8 T_{eff} cells and T_m cells) (**Supplementary Fig. 1a**), which indicated that the translation of *Cd8a* mRNA was highly active in quiescent and activated $CD8^+$ T cells, despite dynamic changes in overall translation status. *Il7r* mRNA (which encodes CD127, a cytokine receptor essential for the maintenance of memory T cells) and *Sell* mRNA (which encodes the lymph-node-homing receptor CD62L) were transcriptionally downregulated in D5 T_{eff} cells and D8 T_{eff} cells relative to their expression in T_n cells and were re-expressed in T_m cells (**Supplementary Fig. 1b**). The amount of individual mRNAs in polysome fractions in T_n cells was indistinguishable from that in those fractions in T_m cells (**Supplementary Fig. 1b**). The transcription of *Gzmb* mRNA (which encodes gramzyme B) was higher D5 T_{eff} cells, D8 T_{eff} cells and T_m cells than in T_n cells (**Supplementary Fig. 1c**). About 50% of the total *Gzmb* mRNA was found in polysome fractions of D5 T_{eff} cells, D8 T_{eff} cells and T_m cells (**Supplementary Fig. 1c**), which suggested that tha translation of *Gzmb* mRNA was similar and active in these cells. Together these results indicated that selective control of translation occurred in activated $CD8^+$ T cells and that the translation of *Ifng* transcripts was dependent on the status of T_{eff} cells.

Defining the translatome of CD8+ T_{eff} cell differentiation

Next, to define the genome-wide control of translation in antigen specific CD8+ T cells after acute infection, we obtained P14 splenic T_n cells, D5 T_{eff} cells and D8 T_{eff} cells from mice (before and after infection with LCMV), isolated polysome-associated mRNA from the cells after sucrose-gradient ultracentrifugation and performed microarray analysis of the mRNA[12], as well as microarray analysis of total mRNA isolated from the same cells before such ultracentrifugation.

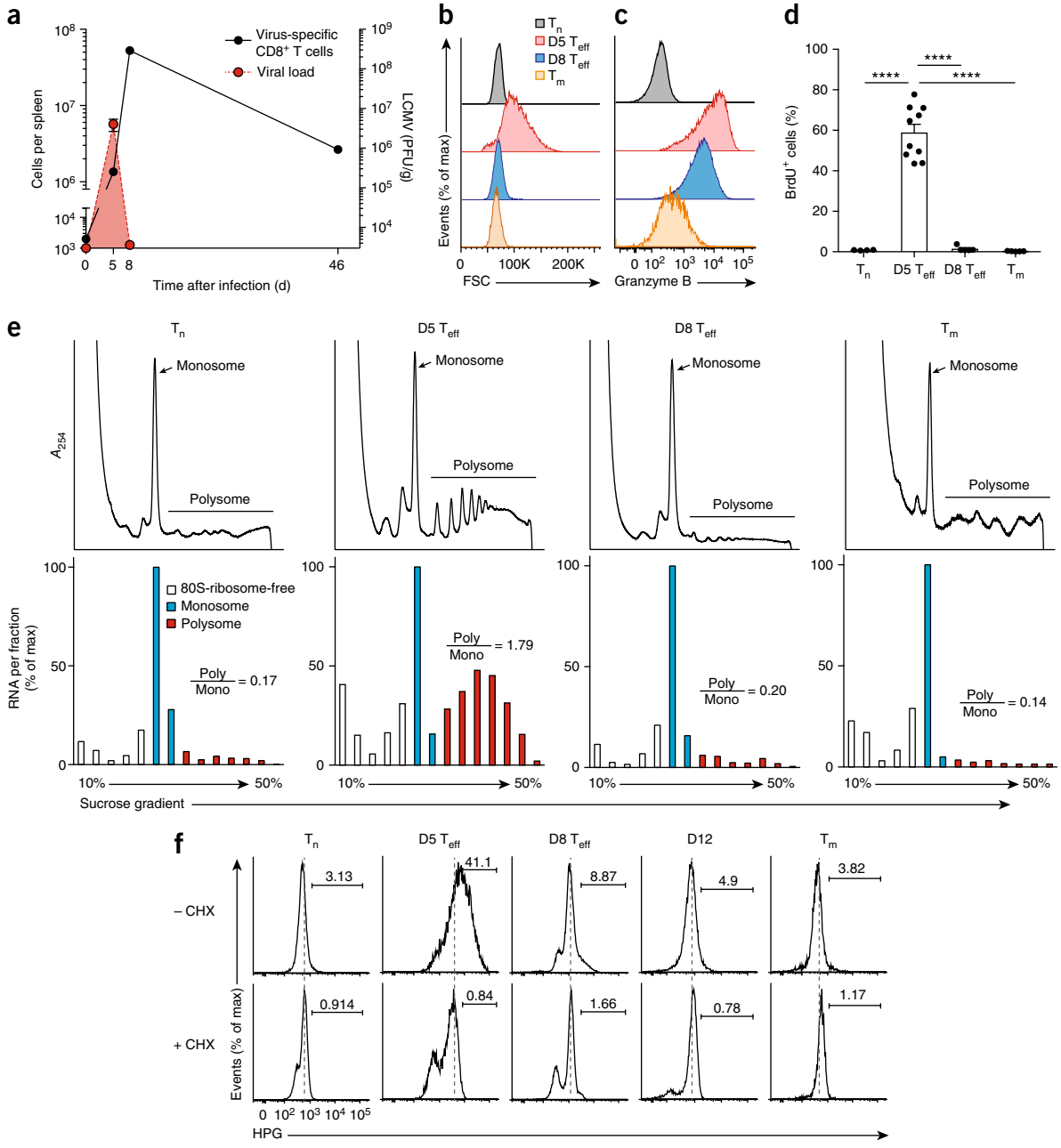

Figure 1 Activated CD8+ T cells change their translational activity. (**a**) Quantification of virus-specific P14 CD8+ T cells (left vertical axis) and viral titers (right vertical axis) in spleen of LCMV-infected mice given adoptive transfer of P14 CD8+ T cells before infection. PFU, plaque-forming units. (**b**,**c**) Cell size (assessed as forward scatter (FSC)) (**b**) and granzyme B expression (**c**) in various P14 CD8+ T cells (key) obtained from the spleen of uninfected or LCMV-infected mice. (**d**) BrdU+ P14 cells in the spleen 2 h after intraperitoneal injection of BrdU into LCMV-infected mice. Each symbol represents an individual mouse. (**e**) Polysome profiles of purified P14 cells in the spleen at various time points (above plots), assessed by sucrose-gradient ultracentrifugation (top row), and quantification of RNA isolated from those gradients (bottom row); numbers in plots (bottom row) indicate the ratio of the amount of RNA in polysomes to that in monosomes (Poly/Mono). Signals observed in polysome fractions of T_m cells are noise due to the much lower number of P14 cells at that point than that at other time points. (**f**) HPG staining in P14 T_n cells, D5 and D8 T_{eff} cells, T cells at day 12 (D12) and T_m cells, among splenocytes cultured for 2 h with HPG in the presence (+CHX) or absence (–CHX) of cycloheximide (left margin). Numbers above bracketed lines indicate percent HPG+ cells. $^{****}P < 0.0001$ (one-way analysis of variance (ANOVA)). Data are representative of at least three independent experiments with samples pooled from three to ten mice per time point (**a**,**e**; mean ± s.e.m. in **a**), are representative of two independent experiments with $n = 3$–6 mice per group (**b**,**c**,**f**) or are from two independent experiments (**d**; mean + s.e.m. of $n = 4$–10 mice per group).

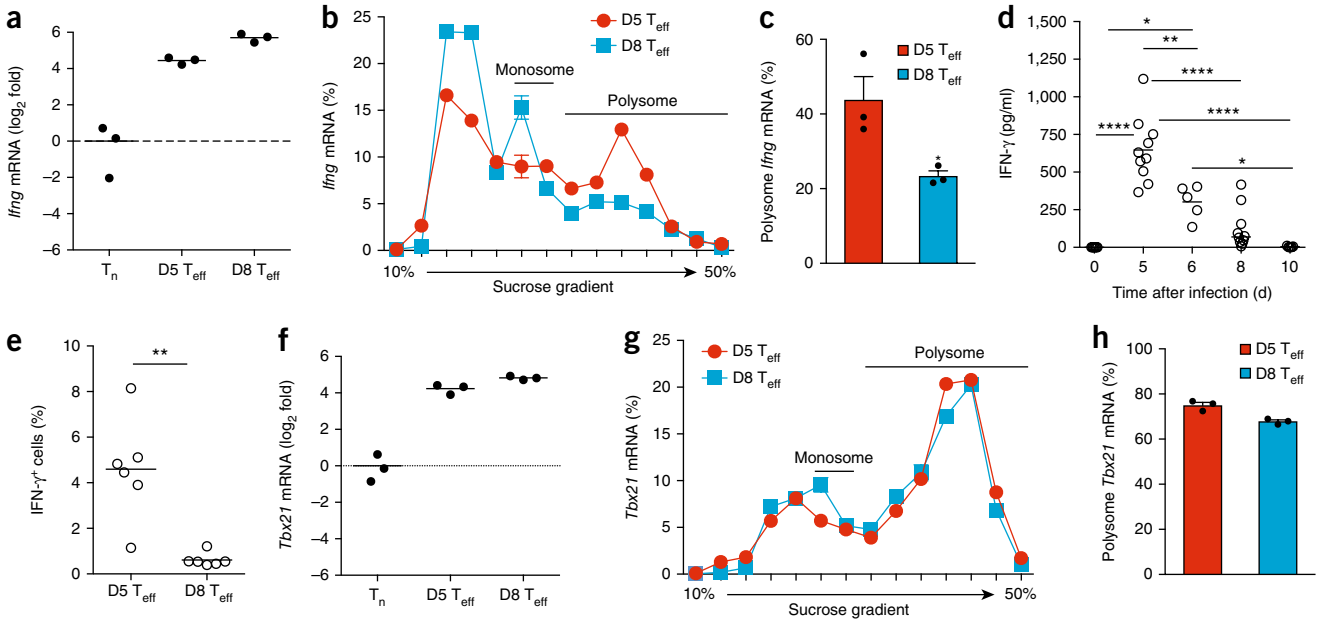

Figure 2 Translation of *Ifng* in CD8$^+$ T_{eff} cells is distinct from that of *Tbx21*. (**a**,**f**) qRT-PCR analysis of *Ifng* mRNA (**a**) and *Tbx21* mRNA (**f**) among total mRNA isolated from P14 T_n cells, D5 T_{eff} cells and D8 T_{eff} cells (horizontal axes) from the spleen; results are presented relative to those of total RNA from T_n cells. (**b**,**c**,**g**,**h**) qRT-PCR quantification of *Ifng* mRNA (**b**) or *Tbx21* mRNA (**g**) in fractions (horizontal axes) obtained by sucrose-gradient ultracentrifugation of lysates of P14 D5 T_{eff} cells and D8 T_{eff} cells (key), among the total in all fractions (**b**,**g**), and the proportion of *Ifng* (**c**) or *Tbx21* (**h**) in the polysome fractions of those cells (key). $^*P < 0.05$ (unpaired *t*-test). (**d**) IFN-γ protein in serum of mice at various times (horizontal axis) after infection with LCMV Arm. $^*P < 0.05$, $^{**}P < 0.01$ and $^{****}P < 0.0001$ (one-way ANOVA). (**e**) Direct *ex vivo* intracellular staining of IFN-γ in splenic P14 D5 T_{eff} cells and D8 T_{eff} cells (horizontal axis), presented as the frequency of IFN-γ$^+$ cells. $^{**}P < 0.01$ (unpaired *t*-test). Each symbol (**a**,**c**,**d**,**e**,**f**,**h**) represents an individual experiment (**a**,**c**,**f**,**h**) or mouse (**d**,**e**); small horizontal lines (**a**,**d**,**e**,**f**) indicate the mean. Data are from three independent experiments (**a**,**c**,**f**,**h**; mean + s.e.m. in **c**,**h**), are representative of three independent experiments with samples pooled from three to ten mice per time point (**b**,**g**; mean ± s.e.m.), are from two independent experiments with $n = 5$–10 mice per time point (**d**) or are representative of two experiments with $n = 6$ mice per time point (**e**).

To obtain basic information of translational control in antigen-specific CD8$^+$ T cells, we plotted the microarray expression values of individual genes in total mRNA against 'translation activity', which represents the recruitment of mRNAs to polysome and was calculated by division of expression values of polysome-associated mRNA by those of total mRNA. In these analyses, four groups were identified (**Fig. 3a** and **Supplementary Tables 1–3**): group I contained mRNAs with low expression and efficient recruitment to polysomes; group II contained mRNAs with low expression and inefficient recruitment to polysomes; group III contained mRNAs with high expression and efficient recruitment to polysomes; and group IV contained mRNAs with high expression and inefficient recruitment to polysomes (**Fig. 3a**). Gene-ontology analysis of these four groups revealed that the pattern of translation activity of T_n cells was more similar to that of D8 T_{eff} cells than to that of D5 T_{eff} cells (**Fig. 3b**). mRNAs that had low expression but were actively translated (group I) in T_n cells and D8 T_{eff} cells encoded products related to multiple biological processes, including 'cellular response to DNA damage' and 'intracellular protein transport' (**Fig. 3b**). On the other hand, mRNAs in group IV (high mRNA expression but inefficient recruitment to polysomes) encoded products associated with 'mitochondrion organization', 'translation-ribosome', and 'oxidative phosphorylation' (**Fig. 3b**). In particular, the translation activity of transcripts encoding products related to translation itself ('translation-ribosome'), which includes mRNAs encoding ribosomal proteins (called 'RP mRNAs' here), was lower in D8 T_{eff} cells than in T_n cells or D5 T_{eff} cells (**Fig. 3b** and **Supplementary Tables 1–3**).

Although the analyses reported above provided basic information on translation activity in CD8$^+$ T_n cells, D5 T_{eff} cells and D8 T_{eff} cells, it was not clear whether and how translation activity of individual mRNAs was altered when T_n cells differentiated into D5 T_{eff} cells and D8 T_{eff} cells. To address this, we compared the expression of total mRNAs in D5 T_{eff} cells and D8 T_{eff} cells relative to that in T_n cells with the same comparison of polysome-associated mRNAs and assessed the relationship of the change in total mRNAs with that in polysome-associated mRNAs. When we compared the microarray data of D5 T_{eff} cells with those of T_n cells, we found a marked correlation between the change in total mRNAs and that in polysome-associated mRNAs (**Fig. 4a**), which indicated that transcriptional regulation was directly related to the amount of polysome-associated mRNA and that the expression changes for the majority of polysome-associated mRNAs could be explained by the increase or decrease in the expression of total mRNA when T_n cells differentiated into D5 T_{eff} cells. There was a similar strong correlation between total mRNAs and polysome-associated mRNAs in terms of such changes in expression in D8 T_{eff} cells relative to that in T_n cells (**Fig. 4a**). Next we quantified genes that were transcriptionally or translationally regulated. We found that 1,932 gene probes were transcriptionally upregulated, 1,975 gene probes were downregulated and 12,001 gene probes were unchanged in D5 T_{eff} cells relative to their expression in T_n cells (**Fig. 4b**). Between 1% and 10% of genes in these three groups were identified as translationally regulated genes, defined as significant up- or downregulation in translational activity (a change in translational activity in D5 T_{eff} cells of less than −1.5 fold or more than 1.5-fold, relative to that

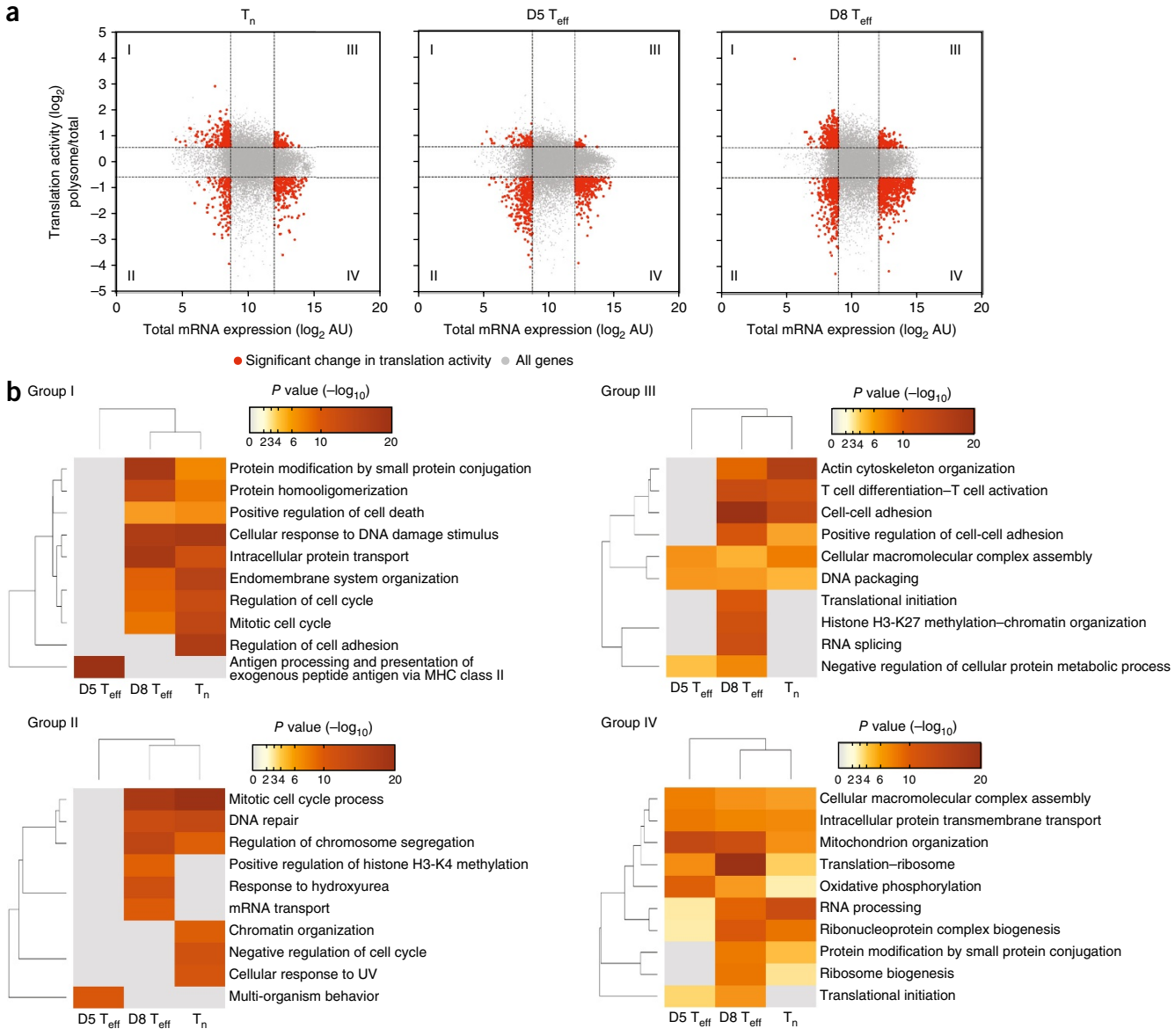

Figure 3 Genome-wide translational activity in CD8⁺ T cells. (**a**) Microarray analysis of RNA isolated from P14 T_n cells, D5 T_{eff} cells and D8 T_{eff} cells (above plots) before and after separation by sucrose-gradient ultracentrifugation, presented as the relationship between expression of total mRNA (microarray data; before ultracentrifugation) and translation activity (calculated by division of microarray values for polysome-associated mRNA (after ultracentrifugation) by those for total mRNA), categorizing genes into four groups (I–IV; as described in Results). AU, arbitrary units. (**b**) Metascape analysis showing the biological processes (right margins) associated with genes in the four groups of genes in **a** (above plots) in P14 D5 T_{eff} cells , D8 T_{eff} cells and T_n cells (below plots); brackets (left margin and top), hierarchical clustering. Data are from three independent experiments with samples pooled from three to ten mice per time point.

in T_n cells) (**Fig. 4b** and **Supplementary Table 4**). Similar to results obtained for D5 T_{eff} cells, the proportion of translationally regulated genes in D8 T_{eff} cells was in the range of about 1–10% (**Fig. 4b** and **Supplementary Table 4**). When comparing the translationally regulated genes in D5 T_{eff} cells with those in D8 T_{eff} cells, we found that the majority of genes were uniquely regulated in each T_{eff} cell population (n = 812 genes for D5 T_{eff} cells, and n = 545 genes for D8 T_{eff} cells; **Fig. 4c**), which suggested that the regulation of mRNA translation in D5 T_{eff} cells was distinct from that in D8 T_{eff} cells.

To define the biological activity and/or the pathways regulated by translation, we used gene-set–enrichment analysis (GSEA)[24] to analyze the expression of total mRNA and polysome-associated mRNA in T_n cells, D5 T_{eff} cells and D8 T_{eff} cells. Mutually overlapping gene sets in GSEA data clustered together, and enrichment data for the GSEA of total mRNA were compared with those of polysome-associated mRNA. This analysis indicated that for total mRNA, D5 T_{eff} cells upregulated (relative to such expression in T_n cells) a substantial number of gene sets encoding products related to cell proliferation and cell division, including 'cell cycle', 'mitosis', 'DNA repair–DNA replication', 'RNA processing', 'transcription', 'splicing', 'DNA metabolism', 'tRNA aminoacylation' and 'chromosome' (**Fig. 5a**), and comparable upregulation was observed for polysome-associated mRNA (**Fig. 5a**); this indicated that the majority of these genes transcriptionally upregulated in D5 T_{eff} cells were loaded onto polysomes. In accordance

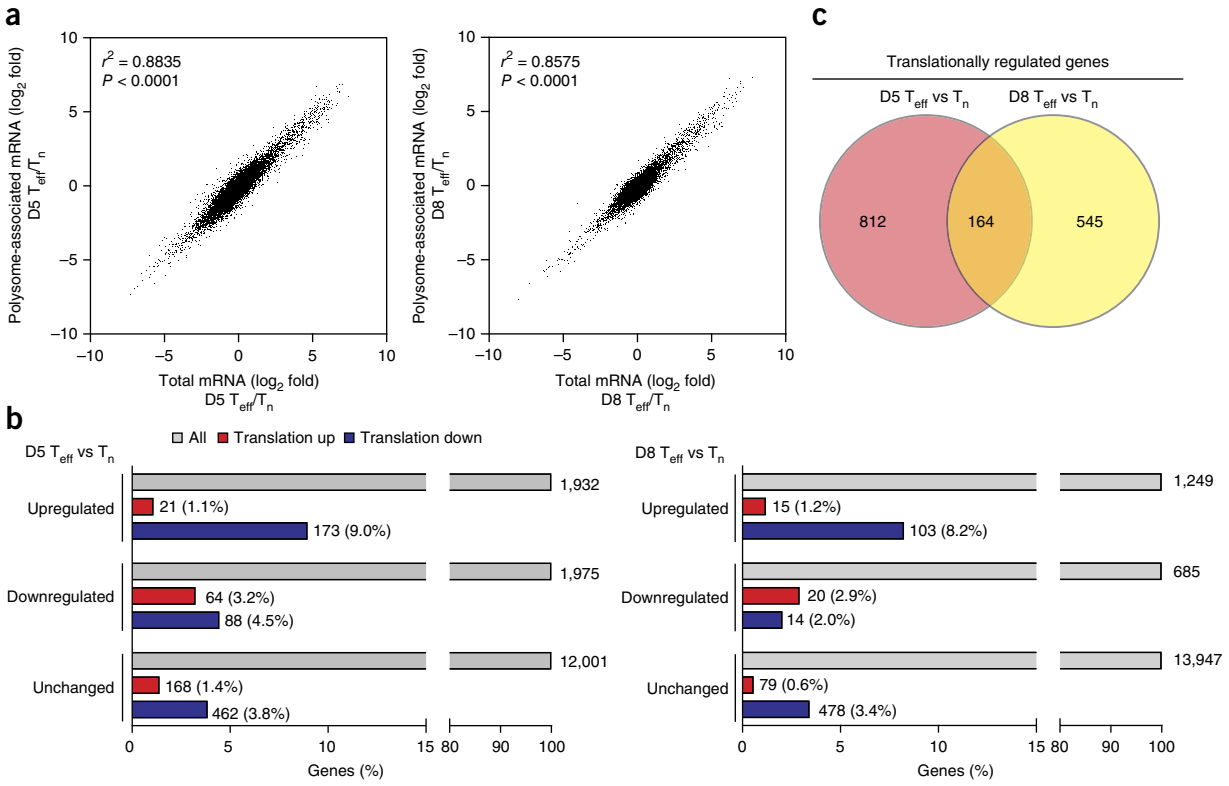

Figure 4 Translatome reveals genes translationally regulated in CD8$^+$ T cells. (**a**) Microarray analysis of RNA isolated from P14 CD8$^+$ T_n cells, D5 T_{eff} cells and D8 T_{eff} cells before and after separation by sucrose-gradient ultracentrifugation, presented as the correlation of the expression of total mRNA (before ultracentrifugation) in T_{eff} cells relative to that of T_n cells (horizontal axes) with that of polysome-associated mRNA (after ultracentrifugation) in T_{eff} cells relative to that of T_n cells (vertical axes), for D5 T_{eff} cells versus T_n cells (left) or D8 T_{eff} cells versus T_n cells (right). Numbers in plots indicate Pearson correlation r^2 values and P values. (**b**) Frequency of translationally regulated genes (change in translation activity of less than −1.5 fold or more than 1.5-fold) (key) among gene probes transcriptionally upregulated (change in expression of over 2-fold), downregulated (change in expression of less than −2-fold) or unchanged in T_{eff} cells relative to their expression in T_n cells (left margin), for D5 T_{eff} cells versus T_n cells (left) or D8 T_{eff} cells versus T_n cells (right); numbers at ends of bars indicate total gene probes (numbers in parentheses indicate frequency). (**c**) Overlap (middle) of genes translationally regulated in D5 T_{eff} cells versus T_n cells (left) and in D8 T_{eff} cells versus T_n cells (right) as identified in **b**. Data are from the microarray data in **Figure 3**.

with that, analysis of mRNAs responsible for the enrichment for these proliferation-related gene sets by GSEA indicated a marked correlation between total mRNAs and polysome-associated mRNAs in terms of such changes (**Supplementary Fig. 2** and **Supplementary Table 5**).

The gene sets encoding products related to cell proliferation and division were also upregulated, as assessed by both total mRNA and polysome-associated mRNA, in D8 T_{eff} cells relative to T_n cells (**Fig. 5a**). However, the number of gene sets upregulated in D8 T_{eff} cells was substantially lower than that in D5 T_{eff} cells (**Fig. 5a**), which suggested that the expression of genes encoding products associated with cell proliferation and division was lower in D8 T_{eff} cells than in D5 T_{eff} cells, as also indicated by direct comparison of D8 T_{eff} cells with D5 T_{eff} cells via GSEA (**Fig. 5a**).

The analyses reported above also revealed significant differences between total mRNA and polysome-associated mRNA in their enrichment, as assessed by GSEA. One noticeable difference was found in the 'ribosome-translation' cluster; downregulation of gene sets encoding products related to this cluster in D8 T_{eff} cells relative to their expression in T_n cells and D5 T_{eff} cells was evident only for polysome-associated mRNA, not total mRNA (**Fig. 5a**), which indicated that the translation of genes encoding products related 'ribosome-translation' was inhibited in D8 T_{eff} cells. Similarly, substantial enrichment for gene sets encoding products related to 'biosynthetic processes and translation initiation' was observed in polysome-associated mRNA relative to total mRNA when microarray data of D8 T_{eff} cells were compared with those of D5 T_{eff} cells (**Fig. 5a**). The significant difference between total mRNA and polysome-associated mRNAs in terms of enrichment for the 'ribosome-translation' cluster was due mostly to translational downregulation of cellular ribosomal proteins in D8 T_{eff} cells relative to their translation in T_n cells and D5 T_{eff} cells (**Fig. 5b** and **Supplementary Table 6**). Similarly, in the 'biosynthetic process and translation initiation' cluster, mRNAs encoding cellular ribosomal proteins were identified as translationally downregulated in D8 T_{eff} cells relative to their translation in D5 T_{eff} cells (**Fig. 5b** and **Supplementary Table 6**).

In addition, when microarray data of D5 T_{eff} cells and D8 T_{eff} cells were analyzed by GSEA, enrichment for a substantial number of 'immune related' gene sets was observed in polysome-associated mRNA relative to total mRNA in D8 T_{eff} cells (**Fig. 5a**). A wide variety of genes, including those encoding transcription factors (*Foxo3*, *Nfat5*, *Stat1* and *Stat5b*), integrins (*Itga1*, *Itgal* and *Itgax*), and kinase or kinase-related molecules (*Pik3ap1*, *Pik3cd*, *Pik3r1* and *Rictor*) were identified as being translationally upregulated in D8 T_{eff} cells relative to their translation in D5 T_{eff} cells (**Supplementary Table 6**). On the basis of analysis by the Metascape gene-annotation and analysis resource, these genes encode products that belong to the categories 'lymphocyte

activation–positive regulation of immune system', 'intracellular signaling–kinase activity' and 'cell adhesion–cell junction' (**Fig. 5c**), which suggested that their translational upregulation might help maintain the cytotoxic activity of CD8$^+$ D8 T_{eff} cells.

To further investigate whether the translation of genes encoding products related to the immune response was regulated differentially in D5 T_{eff} cells than in D8 T_{eff} cells, we performed GSEA using immunology-specific gene sets that can detect an immunological gene signature

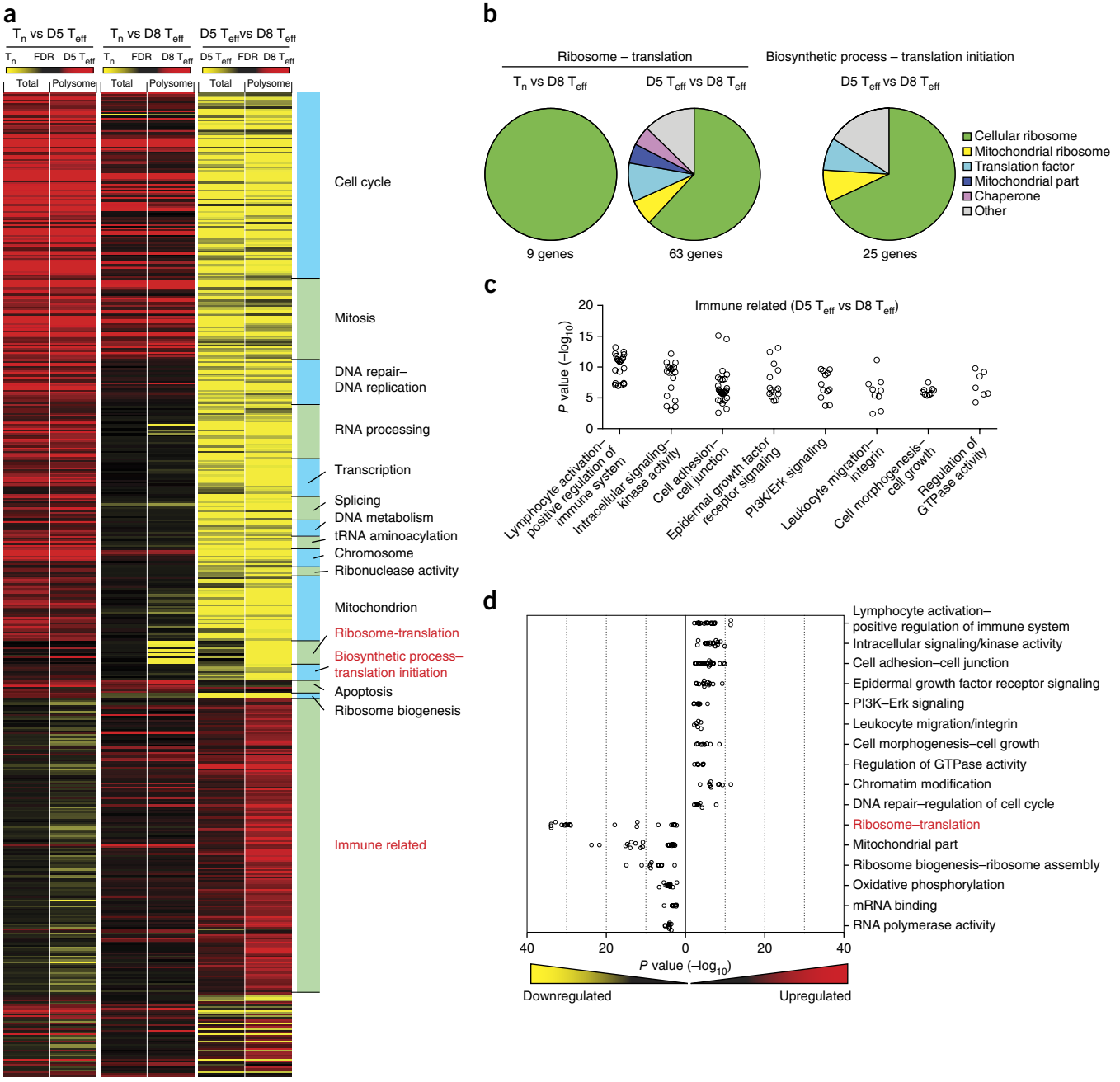

Figure 5 Translational regulation links to cellular activity during the differentiation of CD8$^+$ T_{eff} cells. (**a**) GSEA of total and polysome-associated RNA (above plots) from T_n cells, D5 T_{eff} cells and D8 T_{eff} cells (one gene set per row), presented as the false-discovery rate (FDR) (keys above plots), showing biological 'themes' and pathways (right margin; Molecular Signatures Database) upregulated or downregulated in T_n cells versus D5 T_{eff} cells (left), T_n cells versus D8 T_{eff} cells (middle), or D5 T_{eff} cells versus D8 T_{eff} cells (right); the c2 canonical pathways, c5 gene ontology and hallmark gene sets were combined. (**b**) Proportion of genes encoding products in various categories (key) of the ribosome-translation (left and middle) or biosynthetic process–translation initiation (right) pathways (red in **a**), among genes (totals below plots) translationally downregulated in D8 T_{eff} cells relative to their translation in T_n cells or D5 T_{eff} cells, responsible for the difference in enrichment data between total mRNA and polysome-associated mRNA in T_n cells versus D8 T_{eff} cells (left), D5 T_{eff} cells versus D8 T_{eff} cells (middle), or D5 T_{eff} cells versus D8 T_{eff} cells (right). (**c**) Corresponding gene-ontology terms (below plot), by Metascape analysis, for genes translationally upregulated in D8 T_{eff} cells relative to D5 T_{eff} cells, responsible for the difference in enrichment data between total mRNA and polysome-associated mRNA in D5 T_{eff} cells versus D8 T_{eff} cells (immune related pathway; red in **a**). (**d**) Corresponding gene ontology terms (right margin) for genes translationally up- or downregulated, identified by GSEA with ImmuneSigDB, in D8 T_{eff} cells versus D5 T_{eff} cells (**Supplementary Fig. 3**). Data are from the microarray data in **Figure 3**.

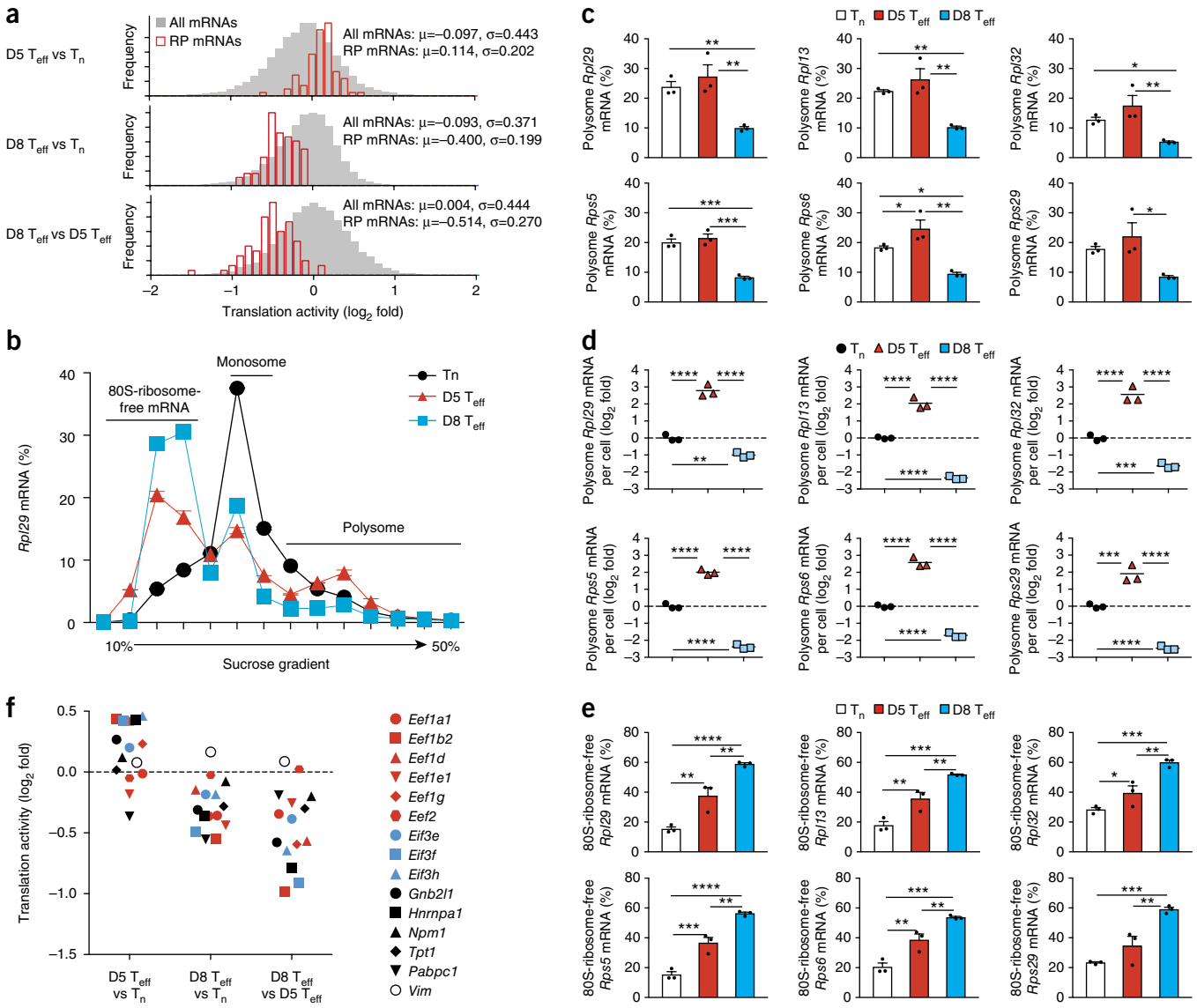

Figure 6 Translational inhibition of RP mRNAs and 5′TOP mRNAs occurs in CD8$^+$ T_{eff} cells when the cells stopped dividing just before the contraction phase. (**a**) Translation activity of all RP mRNAs and of all mRNAs (key) (in the microarray analysis in **Fig. 3**) in D5 T_{eff} cells versus T_n cells (top), D8 T_{eff} cells versus T_n cells cells (middle), and D8 T_{eff} cells versus D5 T_{eff} cells (bottom); numbers in plot indicate the mean (μ) and s.d. (σ). (**b**) qRT-PCR analysis of *Rpl29* mRNA in fractions (horizontal axis) obtained by sucrose-gradient ultracentrifugation of lysates of T_n cells, D5 T_{eff} cells and D8 T_{eff} cells, among the total in all fractions. (**c**) Proportion of RP mRNA in polysome fractions of T_n cells, D5 T_{eff} cells and D8 T_{eff} cells (key). (**d**) Amount of RP mRNA per cell in polysome fractions of T_n cells, D5 T_{eff} cells and D8 T_{eff} cells (key); results are presented relative to those of T_n cells. (**e**) Proportion of 80S-ribosome-free (monosome- and polysome-free) RP mRNA in T_n cells, D5 T_{eff} cells and D8 T_{eff} cells (key). (**f**) Translation activity of 5′TOP mRNAs (other than RP mRNAs; key) in D5 T_{eff} cells versus T_n cells (left), D8 T_{eff} cells versus T_n cells cells (middle), and D8 T_{eff} cells versus D5 T_{eff} cells (right). Each symbol (**c**–**f**) represents an individual experiment (**c**–**e**) or gene (**f**); small horizontal lines (**d**) indicate the mean. $^*P < 0.05$, $^{**}P < 0.01$, $^{***}P < 0.001$ and $^{****}P < 0.0001$ (one-way ANOVA). Data are from the microarray data in **Figure 3** (**a**,**f**) or are representative of (**b**) or from (**c**–**e**) three independent experiments with samples pooled from three to ten mice per group (**b**–**e**; mean ± s.e.m. in **b**,**c**,**e**).

(from the immune signatures of the Molecular Signature Database collection of the GSEA website (ImmuneSigDB))[25]. We found that 150 of 4,872 ImmuneSigDB gene sets were translationally upregulated in D8 T_{eff} cells relative to their translation in D5 T_{eff} cells (**Supplementary Fig. 3**), and the products of genes responsible for this 'enrichment' could be categorized into several biological processes (**Fig. 5d** and **Supplementary Table 6**), including 'chromatin modification' and 'DNA repair–regulation of the cell cycle'. In addition, 60 gene sets were translationally downregulated in D8 T_{eff} cells relative to their translation in D5 T_{eff} cells (**Supplementary Fig. 3**), including genes encoding products related to 'mitochondria', 'ribosome biogenesis–ribosome assembly' and 'oxidative phosphorylation', etc. (**Fig. 5d**). GSEA with ImmuneSigDB also revealed that the translation activity (recruitment of mRNA to polysomes, as defined above) of genes encoding products related to 'ribosome-translation' (mostly RP mRNAs) was much lower in D8 T_{eff} cells than in D5 T_{eff} cells (**Fig. 5d** and **Supplementary Table 6**). These results indicated that the translation of mRNA was dynamically regulated in activated CD8$^+$ T_{eff} cells and that distinct translational programs existed in CD8$^+$ T_{eff} cells at day 5, when cells were actively dividing, and day 8, when cells had stopped proliferating.

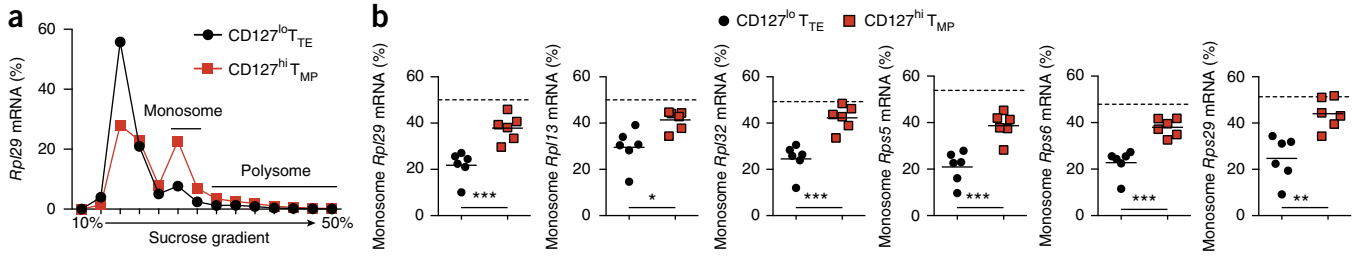

Figure 7 Greater translational inhibition of RP mRNAs in T_{TE} cells than in T_{MP} cells. (**a**) qRT-PCR analysis of *Rpl29* mRNA in fractions obtained by sucrose-gradient ultracentrifugation of P14 CD127^{lo} T_{TE} cells and CD127^{hi} T_{MP} cells (key) (cell purification, **Supplementary Fig. 5**; *Cd8a* mRNA served as a control.). (**b**) Proportion of RP mRNAs in monosome fractions of cells as in **a** (key); dashed horizontal lines indicating the average proportion of each mRNA in monosome fractions in T_n cells (calculated from the data in **Fig. 6**). Each symbol (**b**) represents an individual experiment; small horizontal lines indicate the mean. $*P < 0.05$, $**P < 0.01$ and $***P < 0.001$ (unpaired *t*-test). Data are representative of (**a**) or from (**b**) six independent experiments with samples pooled from three to five mice per group.

Dynamic translational regulation of RP mRNA in T_{eff} cells

Next, to determine if most or only a fraction of mRNAs encoding cellular ribosomal proteins were translationally regulated, we compared the change in the translation of all mRNAs encoding cellular ribosomal proteins with that of all mRNAs in the microarray data. Comparison of translation in D5 T_{eff} cells with that in T_n cells showed that the translation of RP mRNAs relative to that of all mRNAs was modestly upregulated in D5 T_{eff} cells (**Fig. 6a**). On the other hand, the translation of RP mRNA in D8 T_{eff} cells relative to that in T_n cells or D5 T_{eff} cells showed significant downregulation compared with the translation of all mRNAs (**Fig. 6a**). This indicated that the translation of most RP mRNAs was suppressed at the peak of the T_{eff} cell response.

To confirm the microarray results, we obtained T_n cells directly from the spleen of uninfected P14 mice and isolated P14 T_{eff} cells from the spleen of LCMV Arm–infected mice given adoptive transfer of P14 T cells before infection, then assessed (by qRT-PCR) the sedimentation of RP mRNAs in fractions obtained by sucrose-gradient ultracentrifugation of CD8$^+$ T_n cells, D5 T_{eff} cells and D8 T_{eff} cells. About 20% of the total *Rpl29* mRNA (which encodes ribosomal protein L29, one of the components of the large subunit of ribosome) in T_n cells was located in the polysome fractions, and there was a distinct peak of about 40% of the total *Rpl29* in the monosome fraction (**Fig. 6b**,**c**). In D5 T_{eff} cells, the monosome peak became smaller, but the amount of mRNA in the polysome fractions was maintained or was slightly greater than that in T_n cells (**Fig. 6b**,**c**). The amount of *Rpl29* mRNA in polysome fractions was significantly lower in D8 T_{eff} cells than in T_n cells or D5 T_{eff} cells (**Fig. 6b**,**c**). In addition, all RP mRNAs assessed (*Rpl13*, *Rpl32*, *Rps5*, *Rps6* and *Rps29*) showed a significantly lower abundance in the polysome fractions in D8 T_{eff} cells than in those in T_n cells or D5 T_{eff} cells (**Fig. 6c**). The amount of RP mRNA in polysome fractions was also assessed in individual T_n cells, D5 T_{eff} cells and D8 T_{eff} cells. Because the overall RNA content per cell was much higher in D5 T_{eff} cells, due to cell growth and proliferation, the amount of RP mRNA per cell was greater in a D5 T_{eff} cell than in a T_n cell or D8 T_{eff} cell (**Supplementary Fig. 4**). Thus, a D5 T_{eff} cell had significantly higher expression of RP mRNAs in polysome fractions, per cell, than did a T_n cell (**Fig. 6d**). On the other hand, the amount of RP mRNA in polysome fractions per cell was lower in D8 T_{eff} cells than in T_n cells or D5 T_{eff} cells (**Fig. 6d**). Notably, T_n cells had a small amount (about 20%) of 80S-ribosome-free RP mRNAs, while >50% of RP mRNAs were free of 80S ribosome in D8 T_{eff} cells (**Fig. 6b**,**e**), which indicated substantial inhibition of the translation of RP mRNAs in D8 T_{eff} cells.

RP mRNAs contain a 5′ terminal oligopyrimidine tract (5′TOP) sequence that begins with cytosine and is followed by 4–15 pyrimidines, and this motif is involved in translational regulation via mTOR[26–29]. We next sought to determine whether other known 5′TOP mRNAs[26] were also translationally regulated in D5 T_{eff} cells and D8 T_{eff} cells. There was modest upregulation of the translation of other known 5′TOP mRNAs in D5 T_{eff} cells, while their translation was substantially decreased in D8 T_{eff} cells, relative to their translation in T_n cells or D5 T_{eff} cells (**Fig. 6f**), similar to the translational regulation of RP mRNAs. Together these results indicated that the translation of 5′TOP mRNAs, including RP mRNAs, was significantly inhibited in T_{eff} cells when the cells stopped dividing just before the contraction phase.

Distinct translation of RP mRNA in CD8$^+$ T_{TE} and T_{MP} cells

Antigen-specific CD8$^+$ T_{eff} cell populations at day 8 after infection contain CD127^{hi} memory precursor T cells (T_{MP} cells) that differentiate into long-lived CD8$^+$ T_m cells, and CD127^{lo} terminal effector CD8$^+$ T cells (T_{TE} cells) that mostly die during the contraction phase[30–32]. To determine if there were any differences between these two T_{eff} cell subsets in their translational regulation of RP mRNAs, we adoptively transferred P14 T cells into host mice, then purified CD127^{hi} and CD127^{lo} antigen-specific CD8$^+$ P14 T cells from the spleen of the host mice at day 8 after infection with LCMV Arm (**Supplementary Fig. 5a**). CD127^{hi} T_{MP} cells had larger amounts of *Rpl29* mRNA in the monosome fractions than did CD127^{lo} T_{TE} cells (**Fig. 7a**,**b** and **Supplementary Fig. 5b**). Similar observations were made for other RP mRNAs (*Rpl13*, *Rpl32*, *Rps5*, *Rps6* and *Rps29*) (**Fig. 7b**). Although monosomes are often presumed to be translationally inactive, it has been shown that the majority of monosomes actively contribute to translation[33]. The monosome-dependent translation of RP mRNAs in T_{MP} cells might be important for the survival and generation of T_m cells from those cells. Together these results indicated that translational suppression of RP mRNAs was more pronounced in CD8$^+$ T_{TE} cells than in CD8$^+$ T_{MP} cells.

Antigen and mTOR regulate translation of RP mRNA

mTOR regulates the differentiation of CD8$^+$ T_{eff} cells and T_m cells and has an essential role in the translation of 5′TOP mRNAs, including transcripts encoding ribosomal proteins[17–19,26–29]. We next assessed the effect of rapamycin, a specific inhibitor of mTOR, on the translation of RP mRNAs in T_{MP} cells. We adoptively transferred P14 T cells into recipient mice and injected rapamycin into the host mice at day 8 after infection with LCMV Arm, then purified P14 CD127^{hi}

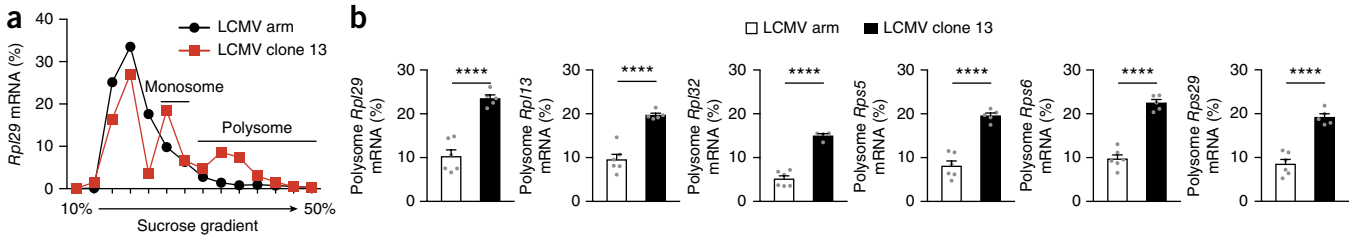

Figure 8 Antigen stimulation contributes to translational regulation of RP mRNAs in virus-specific CD8$^+$ T cells. (**a**) qRT-PCR analysis of *Rpl29* in fractions obtained by sucrose-gradient ultracentrifugation of P14 CD8$^+$ T_{eff} cells collected from the spleen of host mice given adoptive transfer of P14 cells and then infected with either LCMV Arm or LCMV clone 13 (key), assessed at day 8 after infection. (**b**) Proportion of RP mRNA in polysome fractions of D8 T_{eff} cells as in **a**. Each symbol (**b**) represents an individual experiment. $^{****}P < 0.0001$ (unpaired *t*-test). Data are representative of (**a**) or from (**b**) five to six independent experiments with samples pooled from three to five mice per each group (mean + s.e.m. in **b**).

T_{MP} cells 12 h after rapamycin treatment and subjected the cells to sucrose-gradient ultracentrifugation (**Supplementary Fig. 6a**). There was no difference between untreated mice and rapamycin-treated mice in the amount of RP mRNA in the monosome fractions of T_{MP} cells (data not shown), while rapamycin treatment decreased the amount of polysome-associated mRNAs for five of the six RP mRNAs assessed in T_{MP} cells (**Supplementary Fig. 6b**). Next we assessed the effect of rapamycin on the translation of RP mRNAs in antigen-specific CD8$^+$ T cells during early activation. To obtain enough antigen-specific CD8$^+$ T cells for sucrose-gradient ultracentrifugation, we directly infected P14 mice with LCMV Arm in the presence or absence of rapamycin treatment and purified CD8$^+$ T cells from those mice 24 h after infection (**Supplementary Fig. 6c**). Rapamycin treatment significantly decreased the amount of *Rpl13*, *Rpl32* and *Rps5* mRNA in polysome fractions, and the amount of *Rpl29* and *Rps6* mRNAs was also reduced, a result that showed a marginal trend toward significance (**Supplementary Fig. 6d**); this indicated that mTOR signals regulated the translation of RP mRNAs in antigen-specific CD8$^+$ T cells *in vivo*.

To determine whether antigenic stimulation might be involved in translational regulation in activated CD8$^+$ T cells, we adoptively transferred P14 T cells into mice that we then infected with LCMV clone 13 strain, which causes a chronic infection[34]; in this model, persistent antigen continuously stimulates antigen-specific CD8$^+$ T cells, and activated T_{eff} cells gradually differentiate into exhausted T cells. We isolated CD8$^+$ T cells during the acute phase (day 8) of infection with LCMV clone 13, when these CD8$^+$ T cells were still effector cells. As a control, we isolated T_{eff} cells from mice at day 8 after infection with LCMV Arm, when the virus was cleared and thus there was no antigenic stimulation. Sedimentation of RP mRNAs in these cells indicated that translational regulation of such mRNAs in mice infected with LCMV clone 13 was distinct from that of mice infected with LCMV Arm (**Fig. 8a**,**b** and **Supplementary Fig. 7a**,**b**). D8 T_{eff} cells isolated from mice infected with LCMV clone 13 had larger amounts of *Rpl29*, *Rpl13*, *Rpl32*, *Rps5*, *Rps6* and *Rps29* mRNA in the polysome fractions than did such cells from mice infected with LCMV Arm (**Fig. 8a**,**b**). A larger amount of RP mRNA in the polysome fractions was also evident on a per-cell basis in D8 T_{eff} cells isolated from mice infected with LCMV clone 13 than in those from mice infected with LCMV Arm (**Supplementary Fig. 7b**). Together these results indicated that mTOR signals and antigenic stimulation were involved in the translational regulation of RP mRNAs in CD8$^+$ T cells.

DISCUSSION

Here we found that the extent of overall translation in activated CD8$^+$ T cells strongly correlated with cell-proliferation status and was dependent on TCR stimulation. We observed the selective translational control of gene expression in activated CD8$^+$ T cells. The translation of genes such as *Tbx21*, *Cd8a*, *Il7r*, *Sell* and *Gzmb* was efficient throughout the course of CD8$^+$ T cell responses, while the translation of *Ifng* was dynamically altered during T_{eff} cell responses. The translation of RP mRNAs was upregulated in activated CD8$^+$ T cells during the clonal expansion phase, probably to aid the production of larger amounts of proteins in proliferating cells, followed by striking downregulation in the translation of these mRNAs in D8 T_{eff} cells, at the peak of the anti-viral response, even below levels found in T_n cells.

Although neither T_n cells nor D8 T_{eff} cells were dividing, translational suppression of RP mRNAs was evident in D8 T_{eff} cells. The peak of the T_{eff} cell response represents a turning point in metabolic reprogramming in a shift from anabolic processes and rapid cell division to catabolic processes and arrest in cell proliferation accompanied by massive cell death. Thus, the cellular events that trigger this T_{eff} cell death might result in the translational suppression of RP mRNAs. Alternatively, such translational suppression might contribute to the induction of cell death by limiting the availability of ribosomes to synthesize proteins in T_{eff} cells.

T_n cells and T_{MP} cells had large amounts of monosome-associated RP mRNA, but the translation of ribosomal-protein-encoding mRNAs in T_n cells was distinct from that in T_{MP} cells. In particular, the amount of RP mRNA in polysome fractions was substantially lower in T_{MP} cells than in T_n cells. mTOR might be involved in the translational regulation of RP mRNAs. mTOR has two distinct complexes, mTORC1 and mTORC2 (ref. 17). mTORC1 promotes the translation of 5′TOP mRNAs that include transcripts encoding ribosomal proteins[26–29], and our data showed that known 5′TOP mRNAs were translationally suppressed in D8 T_{eff} cells, consistent with mTORC1-mediated inhibition of translation. Furthermore, D8 T_{eff} cells showed downregulation of the translation of genes encoding mitochondria-related proteins, whose translation is regulated at least in part by mTORC1 (refs. 35–38). Thus, our results indicated that inhibition of translation in D8 T_{eff} cells might be dependent on mTORC1 signals. Indeed, rapamycin treatment diminished the amount of ribosomal-protein-encoding mRNA in polysome fractions in antigen-specific CD8$^+$ T cells without changing the amount of monosome-associated RP mRNA. Because inhibition of mTORC1 by rapamycin or RNA-mediated interference promotes the formation of T_m cells[18,19], polysome-dependent translation of RP mRNAs could contribute to the differentiation of T_m cells. An important question is whether and how polysome-dependent translation regulates effector and memory differentiation. Inhibiting mTORC2 signals enhances the generation of CD8$^+$ T_m cells[39,40]. Since mTORC2 can be activated

through interaction with ribosomes[41], the inhibition of polysome-dependent translation of RP mRNAs in D8 T_{eff} cells might lead to limited mTORC2 activity that could have effect on the differentiation of T_m cells. Thus, it will be important to investigate the possible interplay between mTORC1 and mTORC2 during the differentiation of CD8$^+$ T_m cells.

Transcriptional downregulation of a group of RP mRNAs has been reported in exhausted CD8$^+$ T cells that arose after chronic infection[2]. Two distinct subsets of virus-specific CD8$^+$ T cells have been identified during chronic infection: Tim3$^+$TCF1$^-$PD1$^+$ terminally-differentiated exhausted CD8$^+$ T cells, and Tim3$^-$TCF1$^+$PD1$^+$CD8$^+$ T cells with stem-cell-like properties[42–46]. The expression of RP mRNAs was substantially downregulated in Tim3$^+$ TCF1$^-$ PD1$^+$ CD8$^+$ T cells relative to their expression in Tim3$^-$TCF1$^+$PD1$^+$ stem-cell like CD8$^+$ T cells[42,43,46]. In addition, similar transcriptional inhibition of a large number of RP mRNAs has been seen in CD8$^+$ T_m cells repeatedly stimulated with multiple rounds of acute infection[47]. A common feature shared by Tim3$^+$TCF1$^-$PD1$^+$ exhausted T cells and repeatedly stimulated T_m cells is poor proliferative capacity. Because protein synthesis is a key process for T cell proliferation, it seems that transcriptional downregulation of RP mRNAs has a major role in the limited proliferative responses of these CD8$^+$ T cells. Similarly, D8 T_{eff} cells exhibit much lower proliferative capacity than that of T_n cells or primary T_m cells[3]. Thus, the translational downregulation of RP mRNAs in D8 T_{eff} cells might also contribute to poor proliferative responses.

We showed that antigen stimulation and mTOR signals were involved in translational regulation of RP mRNAs in CD8$^+$ T cells. However, translation can be also regulated by other factors. IL-7 might have a role in translational control in CD8$^+$ T cells. T_n cells and T_{MP} cells expressed CD127 (the IL-7 receptor), while T_{TE} cells lost CD127 expression. Our data showed that the amount of monosome-associated RP mRNA was positively correlated with the expression of CD127 when T cells were not stimulated with antigen. In addition, IL-2 might be involved in translational regulation. IL-2 has an essential role in the differentiation of T_{eff} cells and T_m cells[48]. The cytokine receptor IL-2Rα showed transcriptional upregulation in D5 T_{eff} cells in our microarray data, and this increased expression of IL-2Rα was concurrent with the larger amount of polysomes. Furthermore, we found a transcriptional increase in multiple inhibitory receptors, including PD-1, Tim3 and 2B4, in D5 T_{eff} cells and D8 T_{eff} cells. Once antigenic TCR stimulation is lost due to viral clearance, these inhibitory receptors might contribute to translational suppression in D8 T_{eff} cells. Thus, future studies should investigate if such cytokine signals and inhibitory receptors regulate translation in CD8$^+$ T cells.

Translation is a key process in the synthesis of proteins from genetic information encoded in mRNAs. However, protein levels are determined by not only mRNA translation but also rates of protein degradation. A decrease in the translation of a very stable protein in a non-dividing cell would have very little effect on total protein levels. In this situation, translational suppression of such stable protein might be important for maintaining a constant amount of the protein in a cell. Thus, future studies should investigate whether and how the translational regulation defined in the current study is involved in the naive-to-effector differentiation process of virus-specific CD8$^+$ T cells.

In the past two decades, there has been considerable progress in understanding the transcriptional program of the formation of CD8$^+$ T_{eff} and T_m cells, but little is known about translational regulation in antigen-specific CD8$^+$ T cells. Our study provides a framework for understanding the translational control of gene expression when antigen-specific CD8$^+$ T cells are activated *in vivo*.

METHODS

Methods, including statements of data availability and any associated accession codes and references, are available in the online version of the paper.

Note: Any Supplementary Information and Source Data files are available in the online version of the paper.

ACKNOWLEDGMENTS

Supported by the US National Institutes of Health (R01 AI030048 to R.A.) and the Mérieux Foundation (R.A.).

AUTHOR CONTRIBUTIONS

K.A. and R.A. designed the experiments and wrote the paper; M.M. and N.S. provided critical guidance for performing the experiments; K.A., A.G.B. and B.T.K. performed the experiments; and K.A., H.T.K. and R.A. analyzed the data.

COMPETING FINANCIAL INTERESTS

The authors declare no competing financial interests.

1. Kaech, S.M. & Cui, W. Transcriptional control of effector and memory CD8$^+$ T cell differentiation. *Nat. Rev. Immunol.* **12**, 749–761 (2012).
2. Wherry, E.J. *et al.* Molecular signature of CD8$^+$ T cell exhaustion during chronic viral infection. *Immunity* **27**, 670–684 (2007).
3. Kaech, S.M., Hemby, S., Kersh, E. & Ahmed, R. Molecular and functional profiling of memory CD8 T cell differentiation. *Cell* **111**, 837–851 (2002).
4. Russ, B.E. *et al.* Distinct epigenetic signatures delineate transcriptional programs during virus-specific CD8$^+$ T cell differentiation. *Immunity* **41**, 853–865 (2014).
5. Shin, H.M. *et al.* Epigenetic modifications induced by Blimp-1 regulate CD8$^+$ T cell memory progression during acute virus infection. *Immunity* **39**, 661–675 (2013).
6. Scharer, C.D., Barwick, B.G., Youngblood, B.A., Ahmed, R. & Boss, J.M. Global DNA methylation remodeling accompanies CD8 T cell effector function. *J. Immunol.* **191**, 3419–3429 (2013).
7. Youngblood, B. *et al.* Chronic virus infection enforces demethylation of the locus that encodes PD-1 in antigen-specific CD8$^+$ T cells. *Immunity* **35**, 400–412 (2011).
8. Sonenberg, N. & Hinnebusch, A.G. Regulation of translation initiation in eukaryotes: mechanisms and biological targets. *Cell* **136**, 731–745 (2009).
9. Bhat, M. *et al.* Targeting the translation machinery in cancer. *Nat. Rev. Drug Discov.* **14**, 261–278 (2015).
10. Santini, E. & Klann, E. Reciprocal signaling between translational control pathways and synaptic proteins in autism spectrum disorders. *Sci. Signal.* **7**, re10 (2014).
11. Silvera, D., Formenti, S.C. & Schneider, R.J. Translational control in cancer. *Nat. Rev. Cancer* **10**, 254–266 (2010).
12. Piccirillo, C.A., Bjur, E., Topisirovic, I., Sonenberg, N. & Larsson, O. Translational control of immune responses: from transcripts to translatomes. *Nat. Immunol.* **15**, 503–511 (2014).
13. Chang, C.H. *et al.* Posttranscriptional control of T cell effector function by aerobic glycolysis. *Cell* **153**, 1239–1251 (2013).
14. Blagih, J. *et al.* The energy sensor AMPK regulates T cell metabolic adaptation and effector responses in vivo. *Immunity* **42**, 41–54 (2015).
15. Scheu, S. *et al.* Activation of the integrated stress response during T helper cell differentiation. *Nat. Immunol.* **7**, 644–651 (2006).
16. Bjur, E. *et al.* Distinct translational control in CD4$^+$ T cell subsets. *PLoS Genet.* **9**, e1003494 (2013).
17. Zoncu, R., Efeyan, A. & Sabatini, D.M. mTOR: from growth signal integration to cancer, diabetes and ageing. *Nat. Rev. Mol. Cell Biol.* **12**, 21–35 (2011).
18. Araki, K. *et al.* mTOR regulates memory CD8 T-cell differentiation. *Nature* **460**, 108–112 (2009).
19. Pearce, E.L. *et al.* Enhancing CD8 T-cell memory by modulating fatty acid metabolism. *Nature* **460**, 103–107 (2009).
20. Wherry, E.J. *et al.* Lineage relationship and protective immunity of memory CD8$^+$ T cell subsets. *Nat. Immunol.* **4**, 225–234 (2003).
21. Signer, R.A., Magee, J.A., Salic, A. & Morrison, S.J. Haematopoietic stem cells require a highly regulated protein synthesis rate. *Nature* **509**, 49–54 (2014).
22. Narita, M. *et al.* Spatial coupling of mTOR and autophagy augments secretory phenotypes. *Science* **332**, 966–970 (2011).
23. Pien, G.C., Nguyen, K.B., Malmgaard, L., Satoskar, A.R. & Biron, C.A. A unique mechanism for innate cytokine promotion of T cell responses to viral infections. *J. Immunol.* **169**, 5827–5837 (2002).

24. Subramanian, A. *et al.* Gene set enrichment analysis: a knowledge-based approach for interpreting genome-wide expression profiles. *Proc. Natl. Acad. Sci. USA* **102**, 15545–15550 (2005).
25. Godec, J. *et al.* Compendium of immune signatures identifies conserved and species-specific biology in response to inflammation. *Immunity* **44**, 194–206 (2016).
26. Meyuhas, O. & Kahan, T. The race to decipher the top secrets of TOP mRNAs. *Biochim. Biophys. Acta* **1849**, 801–811 (2015).
27. Miloslavski, R. *et al.* Oxygen sufficiency controls TOP mRNA translation via the TSC-Rheb-mTOR pathway in a 4E-BP-independent manner. *J. Mol. Cell Biol.* **6**, 255–266 (2014).
28. Thoreen, C.C. *et al.* A unifying model for mTORC1-mediated regulation of mRNA translation. *Nature* **485**, 109–113 (2012).
29. Hsieh, A.C. *et al.* The translational landscape of mTOR signalling steers cancer initiation and metastasis. *Nature* **485**, 55–61 (2012).
30. Kaech, S.M. *et al.* Selective expression of the interleukin 7 receptor identifies effector CD8 T cells that give rise to long-lived memory cells. *Nat. Immunol.* **4**, 1191–1198 (2003).
31. Joshi, N.S. *et al.* Inflammation directs memory precursor and short-lived effector CD8$^+$ T cell fates via the graded expression of T-bet transcription factor. *Immunity* **27**, 281–295 (2007).
32. Sarkar, S. *et al.* Functional and genomic profiling of effector CD8 T cell subsets with distinct memory fates. *J. Exp. Med.* **205**, 625–640 (2008).
33. Heyer, E.E. & Moore, M.J. Redefining the translational status of 80S monosomes. *Cell* **164**, 757–769 (2016).
34. Wherry, E.J., Blattman, J.N., Murali-Krishna, K., van der Most, R. & Ahmed, R. Viral persistence alters CD8 T-cell immunodominance and tissue distribution and results in distinct stages of functional impairment. *J. Virol.* **77**, 4911–4927 (2003).
35. Morita, M. *et al.* mTORC1 controls mitochondrial activity and biogenesis through 4E-BP-dependent translational regulation. *Cell Metab.* **18**, 698–711 (2013).
36. Larsson, O. *et al.* Distinct perturbation of the translatome by the antidiabetic drug metformin. *Proc. Natl. Acad. Sci. USA* **109**, 8977–8982 (2012).
37. Albert, V. & Hall, M.N. mTOR signaling in cellular and organismal energetics. *Curr. Opin. Cell Biol.* **33**, 55–66 (2015).
38. Chauvin, C. *et al.* Ribosomal protein S6 kinase activity controls the ribosome biogenesis transcriptional program. *Oncogene* **33**, 474–483 (2014).
39. Pollizzi, K.N. *et al.* mTORC1 and mTORC2 selectively regulate CD8$^+$ T cell differentiation. *J. Clin. Invest.* **125**, 2090–2108 (2015).
40. Zhang, L. *et al.* Mammalian target of rapamycin complex 2 controls CD8 T cell memory differentiation in a Foxo1-dependent manner. *Cell Rep.* **14**, 1206–1217 (2016).
41. Zinzalla, V., Stracka, D., Oppliger, W. & Hall, M.N. Activation of mTORC2 by association with the ribosome. *Cell* **144**, 757–768 (2011).
42. He, R. *et al.* Follicular CXCR5- expressing CD8$^+$ T cells curtail chronic viral infection. *Nature* **537**, 412–428 (2016).
43. Im, S.J. *et al.* Defining CD8$^+$ T cells that provide the proliferative burst after PD-1 therapy. *Nature* **537**, 417–421 (2016).
44. Leong, Y.A. *et al.* CXCR5$^+$ follicular cytotoxic T cells control viral infection in B cell follicles. *Nat. Immunol.* **17**, 1187–1196 (2016).
45. Utzschneider, D.T. *et al.* T cell factor 1-expressing memory-like CD8$^+$ T cells sustain the immune response to chronic viral infections. *Immunity* **45**, 415–427 (2016).
46. Wu, T. *et al.* The TCF1-Bcl6 axis counteracts type I interferon to repress exhaustion and maintain T cell stemness. *Science Immunol.* **1**, eaai8593 (2016).
47. Wirth, T.C. *et al.* Repetitive antigen stimulation induces stepwise transcriptome diversification but preserves a core signature of memory CD8$^+$ T cell differentiation. *Immunity* **33**, 128–140 (2010).
48. Chang, J.T., Wherry, E.J. & Goldrath, A.W. Molecular regulation of effector and memory T cell differentiation. *Nat. Immunol.* **15**, 1104–1115 (2014).

ONLINE METHODS

Mice, viral infection, viral titration and measurement of serum IFN-γ. 6- to 12-week old female C57BL/6j (B6) mice were purchased from Jackson laboratories. CD45.1$^+$ or Thy1.1$^+$ P14 mice (which have transgene encoding a TCR specific for the gp33 epitope) were maintained in our animal facility. 1×10^4 to 2×10^4 P14 cells were adoptively transferred into B6 mice, followed by infection with LCMV Armstrong strain (2×10^5 PFU, intraperitoneally). For early activation experiments (**Supplementary Fig. 6c**,**d**), P14 mice were directly infected with LCMV Armstrong strain (2×10^6 PFU, intravenously). For infection with LCMV clone 13, mice that had received 2×10^3 P14 cells were infected intravenously with LCMV clone 13 (2×10^6 PFU). Viral titers in spleen were measured by plaque assay as described previously[34]. Serum IFN-γ was measured by a CBA kit (BD) according to manufacturer's instruction. All animal experiments were approved by the Institutional Animal Care and Use Committee of Emory University.

BrdU labeling and detection. BrdU (1 mg per mouse, Sigma) was injected intraperitoneally into mice, and spleens were harvested from the mice 2 h after BrdU injection. To examine cell proliferation, BrdU incorporation was measured in P14 cells by a BrdU flow kit (BD, catalog#559619).

Polysome profiles. Polysome profiles were analyzed as described previously[49]. In brief, to analyze polysome profiles, P14 cells were purified from spleen. To obtain P14 T_n cells, single-cell suspensions of spleens from uninfected P14 mice were stained with APC-conjugated anti-CD8a (53-6.7, BD), and then CD8$^+$ T cells were isolated by a CD8a$^+$ isolation kit (Miltenyi Biotech). Those CD8$^+$ T cells were further purified by anti-APC MicroBeads (Miltenyi Biotech). For purification of P14 D5 T_{eff} cells, D8 T_{eff} cells and T_m cells, single-cell suspension of spleens from LCMV-infected mice (B6, CD45.2$^+$) given adoptive transfer of P14 (CD45.1$^+$) cells were stained with biotin-conjugated anti-CD45.2 (104, BioLegend), biotin-conjugated anti-Ly6G (1A8, BioLegend) and APC-conjugated anti-CD45.1 (A20, BioLegend). P14 cells were enriched by removing recipient (B6 mice) cells with anti-biotin MicroBeads (Miltenyi Biotech), and then further purification was performed by anti-APC MicroBeads (Miltenyi Biotech). For purification of CD127^{hi} or CD127^{lo} D8 T_{eff} cells, single-cell suspension of spleens from LCMV-infected mice (B6, Thy-1.2) given adoptive transfer of P14 (Thy-1.1$^+$) cells were stained with biotin-conjugated anti-CD127 (A7R34, eBioscience) and APC-conjugated anti-Thy1.1 (OX-7, BioLegend). P14 cells were purified with Anti-APC MultiSort Kit (Miltenyi Biotech), and then further purification was performed by anti-Biotin MicroBeads (Miltenyi Biotech). Dead cells were removed after purification by Percoll density centrifugation. Cycloheximide (100 μg/ml, Sigma) was added to all buffers used during this purification process. Purified P14 cells (>90–95% purity) were lysed; 10% of lysates were used for total RNA analysis, and 90% of the rest of cell lysates were loaded onto 10–50% sucrose gradient, followed by ultracentrifugation as described[49]. After ultracentrifugation, the sucrose gradient was fractionated from the top of the tube. During fractionation, the absorbance was monitored using a UV detector with a 254-nm filter. RNA was isolated from individual fractions using Trizol reagent (Life Technologies). For quantification of RNA, Ribogreen RNA assay kit (Life Technologies) was used, and RNA concentration was determined by NanoDrop 3300 fluorospectrometer.

Protein-synthesis assay. Single-cell suspensions of splenocytes were incubated for 30 min at 37 °C in methionine-free RPMI-1640 medium (Life Technologies) containing 10% dialyzed FBS (Life Technologies), and then were further cultured for 2 h at 37 °C in the presence of HPG (final concentration 100 μM, Life Technologies). Cycloheximide (final concentration 100 μg/ml) was added as a negative control. HPG incorporation into P14 cells was stained with Click-iT Plus Alexa Fluor 488 Picolyl Azide Toolkit (Life Technologies) and was detected by flow cytometry.

qRT-PCR. Total RNA was isolated by Trizol reagent from P14 cell lysates before sucrose-gradient ultracentrifugation. 18s rRNA was used as an internal control of gene expression for total RNA. To examine the sedimentation of mRNAs across the fractions of a sucrose gradient, a standard protocol was applied as described previously[28]. In brief, 10 pg of luciferase RNA (Promega) was added to individual fractions of sucrose gradient for normalization, and then RNA was extracted by Trizol reagent. Primers used in this study for qRT-PCR were QuantiTect primers purchased from Qiagen, except for luciferase primers. The followings are sequences for luciferase primers: forward, 5′-GAGATACGCCCTGGTTCCTG-3′; reverse, 5′-ATAAATAACGCGCCCAACAC-3′. qRT-PCR was carried out by QuantiFast SYBR Green RT-PCR Kit (Qiagen). Values of gene expression determined by qRT-PCR in individual fractions of sucrose gradient were normalized to luciferase quantity, and then distribution of the gene expression in the gradient was plotted. To examine relative copy numbers of RP mRNAs, RNA amount per cell was calculated. In brief, 10 pg of luciferase RNA was added to cell lysates before total RNA isolation for normalization, and then RNA was extracted by Trizol reagent. RNA-extraction efficiency was calculated by qRT-PCR analysis of luciferase RNA, and the RNA amount per cell was determined from the RNA-extraction efficiency, RNA concentration, and initial cell number. qRT-PCR analysis of RP mRNAs was performed using 200 pg of total RNA, and relative copy numbers of these mRNAs per cell was calculated from qRT-PCR data and RNA amount per cell.

Translatome analysis. Total RNA and polysome-associated RNA (three or more ribosomes) from purified P14 cells were isolated by Trizol and then were treated with DNase, followed by RNA purification with columns. Three biological replicates for total and polysome-associated RNA of each time point (T_n cells, D5 T_{eff} cells and D8 T_{eff} cells) were prepared. Amplified cDNAs were generated from those total and polysome-associated RNA samples using Ovation Pico WTA System V2 (Nugen) and were hybridized on mouse 430.2 Affymetrix microarray chips at Dana-Farber Cancer Institute. Prior to analysis, microarray data were preprocessed and normalized with robust multichip averaging in GenePattern (Broad Institute). Microarray data are available at the GEO database (accession code: GSE71643). To determine the pattern of translation in P14 CD8$^+$ T_n cells, D5 T_{eff} cells and D8 T_{eff} cells, expression values for total mRNA obtained by microarray and translation activity were plotted (**Fig. 3a**). Translation activity was calculated by division of expression of polysome-associated mRNA (microarray data) by that of total mRNA (microarray data). High or low expression of genes in total mRNA (horizontal axis) were defined using z-score cut-off of ± 1. To determine significant difference in translation activity, we used a cut-off of a P value of <0.05, an FDR of <0.05, and translation activity values of ± 1.5-fold. Four groups of genes were identified: I, low mRNA expression and efficient recruitment to polysome; II, low mRNA expression and inefficient recruitment to polysomes; III, high mRNA expression and efficient recruitment to polysomes; and IV, high mRNA expression and inefficient recruitment to polysomes. To define transcriptionally up- or downregulated genes (**Fig. 4b**), we used a cut-off of a P value of <0.05, an FDR of <0.05, and a change in expression of over twofold. GSEA analysis was performed in GenePattern[24]. Gene sets used for the GSEA in **Figure 5a** was generated by combining three gene set groups (c2 canonical pathways, c5 GO, and hallmark gene-sets) obtained from GSEA Molecular Signatures Database. Gene-sets used in **Figure 5d** and **Supplementary Figure 3** were c7 ImmuneSigDB from GSEA Molecular Signatures Database. In these GSEA analyses, we used a cut-off of an FDR of <0.01 and a P value of <0.001. Mutually overlapping gene-sets in GSEA data were clustered together using Enrichment Map and Auto Annotate programs on a Cytoscape software[50]. These gene-set cluster data made in Cytoscape were further visualized with a heat map in which FDR values were plotted. Translationally regulated gene sets were determined when FDR values of GSEA data for polysome-associated RNA were less than 1/100 relative to those for total RNA. To identify translationally up- or downregulated genes responsible for the difference in enrichment data between total mRNA and polysome-associated mRNA (**Fig. 5**), we determined leading-edge genes in translationally regulated gene sets of polysome-associated RNA microarray data. The leading-edge genes are a core group of genes essential for the gene-set–enrichment signal. From these leading-edge genes, translationally regulated genes were further extracted. Translationally regulated genes were defined as below. First, translational activity for each gene was calculated as (polysome-associated RNA microarray expression value) / (total RNA microarray expression value). Second, values of the translation activity from biological replicates were averaged, and then the change in translation activity (fold values) was calculated for two

doi:10.1038/ni.3795

different stages of $CD8^+$ T cells (for example, T_n cells versus D8 T_{eff} cells). Third, *P* values of the change in translation activity between two different stages were determined by a two-tailed Student's *t*-test, and then FDR was calculated by qvalue program in R software. Finally, we used a cut-off of a *P* value of <0.05, an FDR of <0.15, and a changes of translation activity of >1.5-fold or <-1.5-fold to define a translationally regulated gene. In **Figures 3** and **5c**,**d**, the translationally regulated genes were further analyzed by Metascape (http://metascape.org/gp/index.html#/main/step1) to determine gene-ontology categories overrepresented in a set of genes[51].

Rapamycin administration. Rapamycin was injected intraperitoneally into mice. As previously published[18], 600 μg/kg of rapamycin was administered at day 8 after infection (**Supplementary Fig. 6a**,**b**), and 75 μg/kg of rapamycin was injected 12 h before and after infection (**Supplementary Fig. 6c**,**d**).

Flow cytometry. Flow cytometry was performed with an LSR II or FACSCanto II (BD Biosciences). Single-cell suspensions of spleen cells and peripheral blood mononuclear cells were prepared, and cell surface staining was carried out as shown previously[20]. The following antibodies were purchased from BD Biosciences: anti-CD8a (53-6.7), anti-IFN-γ (XMG1.2), and isotype-matched control antibody for IFN-γ (R3-34). Anti-KLRG1 (2F1) antibody was purchased from SouthernBiotech. Anti-CD127 (A7R34) was purchased from eBioscience. Anti-CD45.1 (A20), anti-CD45.2 (104), anti-Thy-1.1 (OX-7) and anti-Ly6G (1A8) were purchased from BioLegend. For direct *ex vivo* intracellular IFN-γ staining, cell-surface staining of spleen cells was performed to detect P14 cells, and then spleen cells were stained with anti-IFN-γ (identified above) after permeabilization. Isotype-matched control antibody for IFN-γ (identified above) was used to determine the background.

Statistical analysis. *P* values were determined by a two-tailed unpaired or paired Student's *t*-test for comparison of two groups. To compare three or more groups, one-way ANOVA was used to calculate *P* values. Pearson correlation analysis was performed in **Figure 4a** and **Supplementary Figure 2**. Statistical values in GSEA and Metascape were calculated in individual programs.

Data availability. The data that support the findings of this study are available from the corresponding author upon request. GEO accession code for microarray data: GSE71643.

49. Colina, R. *et al.* Translational control of the innate immune response through IRF-7. *Nature* **452**, 323–328 (2008).
50. Merico, D., Isserlin, R., Stueker, O., Emili, A. & Bader, G.D. Enrichment map: a network-based method for gene-set enrichment visualization and interpretation. *PLoS One* **5**, e13984 (2010).
51. Tripathi, S. *et al.* Meta- and orthogonal integration of influenza "OMICs" data defines a role for ubr4 in virus budding. *Cell Host Microbe* **18**, 723–735 (2015).